JM070383C

Supporting Information

Structure-Based Design of Flavonoid Compounds As a New Class Small-Molecule Inhibitors of the Antiapoptotic Bcl-2 Proteins[^]

Guozhi Tang[+], Ke Ding[+], Zaneta Nikolovska-Coleska[+], Chao-Yie Yang[+], Su Qiu[+], Sanjeev Shangary[+], Renxiao Wang[+], Jie Guo[+], Wei Gao[+], Jennifer Meagher[∃], Jeanne Stuckey[∃], Krzysztof Krajewski[#], Sheng Jiang[#], Peter P. Roller[#], Shaomeng Wang[+,]*

[+] Comprehensive Cancer Center and Departments of Internal Medicine, Pharmacology and Medicinal Chemistry, and [∃]Life Sciences Institute, University of Michigan, 1500 E. Medical Center Drive, Ann Arbor, MI 48109, USA;

[#]Laboratory of Medicinal Chemistry, National Cancer Institute-Frederick, National Institutes of Health, Frederick, Maryland 21702;

I. Chemistry

Elemental analyses of compounds 2, 4, 5 and 6.

Comp.	Formula	C%		H%		N%	
		Calc.	Found	Calc.	Found	Calc.	Found
2	$C_{14}H_{16}O_5$	63.63	63.43	6.10	6.23		undetectable
4	$C_{34}H_{34}O_{10}$	67.76	67.53	5.69	5.66		ibid.
5	$C_{20}H_{20}O_5$	70.57	70.37	5.92	6.16		ibid.
6	$C_{40}H_{46}O_{10}$	69.95	69.83	6.75	6.77		ibid.

Solvents and reagents were obtained commercially and were used without further purification. All reactions were carried out under inert atmosphere (N_2) and at room temperature unless otherwise noted. Anhydrous CH_2Cl_2 was distilled from calcium hydride. BBr_3 solution (1M) in CH_2Cl_2 was fresh prepared in lab and used in several days. All reported yields are of isolated products and are optimized. Reactions were monitored by TLC carried out on 250 μm E. Merck silica gel plates (60F-254) using UV light as visualizing agent. E. Merck silica gel (60, particle size 15-40 μm) was used for flash column chromatography. NMR spectra were recorded on a Bruker Avance300 spectrometer (300 MHz). Chemical shifts (δ) are reported as δ values (ppm) downfield relative to TMS as an internal standard, with multiplicities reported in the usual manner. High resolution electrospray ionization mass spectra (MS) were run on a Micromass AutoSpec Ultima mass spectrometer. Elemental analysis (EA) was performed by the Department of Chemistry, University of Michigan (Ann Arbor) using a Perkin-Elmer 2400 Series II Analyzer.

1-(6-hydroxy-2,3,4-trimethoxyphenyl)-2-methylpropan-1-one (7). 5.8 mL of isobutyryl chloride (55.0 mmol) was added into a solution of 3,4,5-trimethoxyphenol (9.21 g, 50.0 mmol) and $BF_3{\cdot}Et_2O$ (35 mL, 275.0 mmol) in 100 mL of anhydrous 1,2-dichloroethane. After refluxing for 12 hours, the mixture was evaporated *in vacuo*. The residue was partitioned between CH_2Cl_2 and HCl (3M), and stirred for 3 hours. The organic phase was washed with brine, and dried over anhydrous Na_2SO_4. Flash chromatography (hexane/EtOAc, 3:1) gave **7** as white solid (10.8 g, 85%). ^{1}H NMR ($CDCl_3$) δ 13.40 (s, 1H), 6.25 (s, 1H), 4.00 (s, 3H), 3.88 (s, 3H), 3.78 (s, 3H), 3.73 (septet, J = 6.8 Hz, 1H), 1.19 (d, J = 6.8 Hz, 6H); ^{13}C NMR ($CDCl_3$) δ 210.7, 162.0; 159.6; 154.9; 134.6; 107.4; 96.2; 61.5; 60.9; 56.0; 39.0; 19.5.

2-Isobutyl-3,4,5-trimethoxy-phenol (8). 20 mL of triethylsilane (125.0 mmol) was added dropwise into a solution of **7** (12.7 g, 50.0 mmol) in 75 mL of TFA. After stirring overnight, the reactants were concentrated *in vacuo*. The residue was purified by silica gel column chromatography (hexane/EtOAc, 4:1) to give **8** as colorless liquid (11.4 g, 95%). ^{1}H NMR ($CDCl_3$) δ 6.21 (s, 1H), 4.76 (br, 1H), 3.87 (s, 3H), 3.80 (s, 3H), 3.79 (s, 3H), 2.41 (d, J = 7.3 Hz, 2H), 1.85 (m, J = 6.8 Hz, 1H), 0.93 (d, J = 6.6 Hz, 6H).

1-(2-Hydroxy-3-isobutyl-4,5,6-trimethoxy-phenyl)-ethanone (9). 0.8 mL of acetyl chloride (11.0 mmol) was added into a solution of **8** (2.4 g, 10.0 mmol) and $BF_3{\cdot}Et_2O$ (6.3 mL, 50.0 mmol) in 60 mL of anhydrous 1,2-dichloroethane. The resulting mixture was refluxed overnight before concentrated *in vacuo*. The residue was dissolved in CH_2Cl_2, and stirred with 30 mL of HCl (3.0 M) for 2 hours. The aqueous phase was extracted with CH_2Cl_2. The organic phases were combined, washed with brine, dried over Na_2SO_4, and evaporated. Acetophenol **9** (2.46 g, 87%) was obtained after chromatography (hexane/EtOAc, 8:1) purification. ^{1}H NMR ($CDCl_3$) δ 13.27 (s, 1H), 3.98 (s, 3H), 3.95 (s, 3H), 3.78 (s, 3H), 2.67 (s, 3H), 2.47 (d, J = 7.3 Hz, 2H), 1.91 (m, J = 6.8 Hz, 1H), 0.90 (d, J = 6.6 Hz, 6H); ^{13}C NMR ($CDCl_3$) δ 200.4, 154.2, 149.6, 143.7, 141.0, 124.6, 124.4, 61.7, 60.9, 60.7, 33.5, 31.7, 28.8, 22.6; MS (Na^+ added) calcd for $C_{15}H_{22}O_5Na^+$: 305.1365; found: 305.1373.

8-Isobutyl-5,6,7-trimethoxy-2-methyl-chromen-4-one (10). Ac_2O (1.9 mL, 40.0 mmol) was added dropwise into a solution of **9** (5.65 g, 20.0 mmol) in 30 mL of anhydrous pyridine. The mixture was concentrated *in vacuo* after overnight stirring. The residue was dissolved in EtOAc, washed with H_2O, HCl (0.1M) and brine, dried over anhydrous Na_2SO_4 and concentrated. The crude product was dissolved in 30 mL of anhydrous DMF and added dropwise into a suspension of NaH (60%, 1.8 g, 44 mmol) in 40 mL of anhydrous DMF at 0 ^oC. The resulted mixture was stirred at room temperature for 6 hours, before quenched with 4 mL of AcOH. The DMF solution was partitioned between large volume of H_2O and EtOAc, and the aqueous phase was extracted twice with EtOAc. The combined organic phases were washed with H_2O and brine, and concentrated. The residue was dissolved in 40 mL of methanol. 5 mL of conc. HCl was added into the solution at 0 ^oC. After stirring overnight at room temperature, the solution was evaporated *in vacuo*. The residue was dissolved in EtOAc, washed with brine, dried over Na_2SO_4 and concentrated. Flash chromatography (hexane/EtOAc, 2:1) afforded 5.0 g of **10** as white solid. The total yield is about 82% for 3 steps. ^1H NMR ($CDCl_3$) δ 6.03 (s, 1H), 4.00 (s, 3H), 3.95 (s, 3H), 3.93 (s, 3H), 2.68 (d, J = 7.2 Hz, 2H), 2.32 (s, 3H), 1.92 (m, J = 6.8 Hz, 1H), 0.95 (d, J = 6.7 Hz, 6H); ^{13}C NMR ($CDCl_3$) δ 177.9, 163.7, 156.1, 152.3, 151.0, 143.7, 119.5, 114.7, 111.0, 62.2, 61.4, 61.3, 32.6, 29.1, 22.8, 20.0.

5,6,7-trihydroxy-8-isobutyl-2-methyl-4H-chromen-4-one (2). 6.0 mL of BBr_3 solution (1.0 M in CH_2Cl_2, 6.0 mmol) was added dropwise into a solution of **10** (306 mg, 1.0 mmol) in 20 mL of anhydrous CH_2Cl_2 at -78 ^oC. The mixture was allowed to warm up to -10 ^oC in a couple of hours. MeOH (2.0 mL) was added into reaction flask to quench the reaction and the mixture was partitioned between H_2O and CH_2Cl_2. The organic phase was washed with H_2O and brine, dried over Na_2SO_4, and concentrated. The residue was purified by flash chromatography (hexane/acetone, 3:1) to give **2** as pale yellowish powder (185 mg, 70%). ^1H NMR (DMSO-d_6) δ 12.77 (s, 1H), 9.78 (s, 1H), 9.07 (s, 1H), 6.13 (s, 1H), 2.55 (d, J = 7.20 Hz, 2H), 2.38 (s, 3H), 1.93-1.84 (m, 1H), 0.86 (d, J = 6.65 Hz, 6H); ^{13}C NMR (DMSO-d_6) δ 183.4, 168.1, 152.7, 149.4, 145.9, 129.1, 107.9, 106.8, 104.1, 32.2, 28.9, 23.3, 20.9; MS (H^+ added) calcd for $C_{14}H_{16}O_5H^+$: 265.1076; found: 265.1077; EA calcd C, 63.63; H, 6.10; found: C, 63.43; H, 6.23.

3-Iodo-8-isobutyl-5,6,7-trimethoxy-2-methyl-chromen-4-one (11). A solution of iodine (4.6 g, 18 mmol) in CH_2Cl_2 was added dropwise to a suspension of CF_3CO_2Ag (5.0 g, 22.5 mmol) and **10** (4.6 g, 15.0 mmol) in 80 mL of CH_2Cl_2 at 0 ^oC. The resulting mixture was stirred for one extra hour before filtered through Celite. The filtrate was washed with 30 mL of saturated $Na_2S_2O_3$ solution and brine, dried over Na_2SO_4, and concentrated *in vacuo*. The residue was purified by silica gel column chromatography (hexane/EtOAc, 4:1) to give iodide **11** as liquid (6.1 g, 94%). ^1H NMR ($CDCl_3$) δ 4.00 (s, 3H), 3.95 (s, 3H), 3.91 (s, 3H), 2.72 (s, 3H), 2.66 (d, J = 7.2 Hz, 2H), 1.90 (m, J = 6.8 Hz, 1H), 0.93 (d, J = 6.7 Hz, 6H); ^{13}C NMR ($CDCl_3$) δ 172.4, 164.1, 156.4, 151.3, 150.7, 144.1, 119.0, 111.4, 89.8, 62.2, 61.3, 61.2, 32.6, 29.0, 25.2, 22.7.

8-isobutyl-5,6,7-trimethoxy-2-methyl-3-phenyl-4H-chromen-4-one (12). 10.0 mL of DMF, 5.0 mL of EtOH, and 3.0 mL of H_2O were transferred into a reaction flask containing iodide **11** (0.65 g, 1.5 mmol), phenylboronic acid (244 mg, 2.0 mmol), Na_2CO_3 (0.32 g, 3.0 mmol) and $Pd_2(dpf)_2Cl_2{\cdot}CH_2Cl_2$ (100 mg). The reactants were stirred at 60 ^oC overnight before concentrated *in vacuo*. The residue was purified by silica gel column chromatography (hexane/EtOAc = 2:1) to give **6** as white solid (0.53 g, 92%). ^1H NMR ($CDCl_3$) δ 7.44-7.38 (m, 2H), 7.36-7.33 (m, 1H), 7.29-7.27 (m, 2H), 4.00 (s, 3H), 3.92 (s, 3H), 3.91 (s, 3H), 2.70 (d, J = 7.2 Hz, 2H), 2.26 (s, 3H), 1.97 (m, J = 6.8 Hz, 1H), 0.97 (d, J = 6.6 Hz, 6H); ^{13}C NMR ($CDCl_3$) δ 176.2, 161.0, 156.0, 151.6, 151.2, 143.8, 133.3, 130.6, 128.3, 127.6, 123.4, 119.2, 114.6, 62.1, 61.3, 61.2, 32.5, 29.0, 22.8, 19.1; MS (Na^+ added) calcd for $C_{23}H_{26}O_5Na^+$: 405.1678; found: 405.1668.

5,6,7-Trihydroxy-8-isobutyl-2-methyl-3-phenyl-chromen-4-one (5). Compound **5** was made by following the same demethylation procedure described for **2** (80% yield). **5** is light yellowish solid. ^1H NMR ($CDCl_3$) δ 12.83 (s, 1H), 7.51-7.28 (m, 5H), 6.15 (s, 1H), 5.49 (s, 1H), 2.71 (d, J = 7.2 Hz, 2H), 2.34 (s, 3H), 2.05-2.01 (m, 1H), 0.98 (d, J = 6.7 Hz, 6H); ^{13}C NMR ($CDCl_3$) δ 181.6, 164.1, 148.9, 143.8, 132.1, 130.4, 128.5, 128.0, 126.8, 121.0, 110.6, 106.3, 104.3, 31.4, 28.6, 22.6, 19.5; MS (H^+ added) calcd for

$C_{20}H_{20}O_5H^+$: 341.1389; found: 341.1384; EA calcd C, 70.57, H, 5.92; found C, 70.37, H, 6.16.

1,4-Bis(5,6,7-trimethoxy-8-isobutyl-2-methyl-4-oxo-4H-chromen-3-yl)benzene (6). Iodide **11** (0.86 g, 2.0 mmol), 1,4-Phenylenebisboronic acid (0.17 g, 1.0 mmol), Na_2CO_3 (0.25 g, 2.4 mmol) and $Pd_2(dpf)_2Cl_2 \cdot CH_2Cl_2$ (100 mg) was added into a flask. 10.0 mL of DMF, 5.0 mL of EtOH, and 3.0 mL of H_2O were transferred into the flask. The resulting mixture was stirred at 90 ^oC for 10 hours before evaporated *in vacuo*. Flash chromatography (hexane/EtOAc = 1:1) gave **6** as white solid (0.66 g, 96%). ^1H NMR ($CDCl_3$) δ 7.36 (s, 4H), 4.01 (s, 6H), 3.95 (s, 6H), 3.93 (s, 6H), 2.71 (d, J = 7.2 Hz, 4H), 2.33 (s, 6H), 1.97 (m, J = 6.7 Hz, 2H), 0.98 (d, J = 6.6 Hz, 12H); ^1H NMR (DMSO-d_6) δ 7.37 (s, 4H), 3.96 (s, 6H), 3.90 (s, 6H), 3.87 (s, 6H), 2.72 (d, J = 7.2 Hz, 4H), 2.33 (s, 6H), 2.06-1.95 (m, 2H), 0.99 (d, J = 6.6 Hz, 12H); ^{13}C NMR ($CDCl_3$) δ 175.9, 161.0, 155.8, 151.3, 150.9, 143.4, 132.1, 130.2, 122.9, 118.9, 114.3, 61.7, 60.9, 60.9, 32.2, 28.7, 22.4, 19.0; MS (Na^+ added) calcd for $C_{40}H_{46}O_{10}Na^+$: 709.2989; found: 709.3011; EA calcd C, 69.95, H, 6.75; found: C, 69.83, H, 6.77.

1,4-Bis(5,6,7-trihydroxy-8-isobutyl-2-methyl-4-oxo-4H-chromen-3-yl)benzene (4). 7.5 mL of BBr_3 solution (1.0 M in CH_2Cl_2) was added dropwise into a solution of **6** (343 mg, 0.5 mmol) in 25 mL of anhydrous CH_2Cl_2 at -78 ^oC. The mixture was allowed to warm to 0 ^oC gradually in a couple of hours. MeOH (2.5 mL) was added into reaction flask to quench the reaction and the mixture was partitioned between H_2O and CH_2Cl_2. The organic phase was washed with H_2O several times, dried over Na_2SO_4, and concentrated. The residue was purified by recrystallization from acetone to give of **4** as pale yellowish solid (217 mg, 72%). ^1H NMR ($CO(CD_3)_2$) δ 7.46 (s, 4H), 2.74 (d, J = 7.2 Hz, 4H), 2.42 (s, 6H), 2.06 (m, 2H), 0.97 (d, J = 6.7 Hz, 12H); ^{13}C NMR ($CO(CD_3)_2$) δ 182.1, 165.0, 151.7, 149.5, 145.7, 133.0, 131.4, 128.6, 121.2, 106.8, 104.6, 32.2, 22.9, 19.7; MS (Na^+ added) calcd for $C_{34}H_{34}O_{10}Na^+$: 625.2050; found: 625.2054; EA calcd C, 67.76, H, 5.69; found: C, 67.53, H, 5.66.

II. Fluorescence-Polarization-based Competitive Binding Assays for Bcl-2, Bcl-xL and Mcl-1 proteins

Protein expression and purification

Human Bcl-2 protein. The isoform 2 construct of the human Bcl-2 with an N-terminal 6xHis tag was used.[0] Bcl-2 protein was produced in *E. coli* BL21(DE3) cells. Cells were grown at 37°C in 2xYT containing antibiotics to an OD_{600} of 0.6. Protein expression was induced by 0.4 mM IPTG at 20°C for 20 h. Cells were lysed in 50mM Tris pH 8.0 buffer containing 500 mM NaCl, 0.1%bME and 40 μl of Leupectin/Aprotin. The protein was purified from the soluble fraction using Ni-NTA resin (QIAGEN), following the manufacturer's instructions. The protein was further purified on a Superdex75 column (Amersham Biosciences) in 25mM Tris pH 8.0 buffer containing 150 mM NaCl and 2 mM DTT.

Human Bcl-xL protein. Human Bcl-xL protein, which has an internal deletion for the 45-85 amino acid residues and a C-terminal truncation for the amino acid residues 212-233, was cloned into the pHis-TEV vector (a modified pET vector). Protein was produced in *E. coli* BL21(DE3) cells with an N-terminal 8xHis tag. Cells were grown at 37°C in 2xYT containing antibiotics to an OD_{600} of 0.6. Protein expression was induced by 0.4 mM IPTG at 25°C for 16 h. Cells were lysed in 50mM Tris, pH7.5 buffer containing 200mM NaCl, 0.1%bME and Leupectin/Aprotin. His-TEV-Bcl-xL protein was purified from the soluble fraction using Ni-NTA resin (QIAGEN), following the manufacturer's instructions. The His-TEV-Bcl-xL protein was further purified on a Superdex75 column

(Amersham Biosciences) in 20mM Tris pH7.5 buffer containing 150mM NaCl and 5mM DTT.

Human Mcl-1 protein. Human Mcl-1 cDNA was purchased from Origene. The Mcl-1 fragment, amino acid residues 171-327, was cloned into the pHis-TEV vector (a modified pET vector) through BamHI and EcoRI sites, using the oligonucleotides: 5'-CGGGATCCGAGGACGAGTTGTACCG-GCAG-3' and 5'-GGAATTCCTAGCCACCTTCTAGGTCCTCTAC-3'. Mcl-1 protein with a N-terminal 8xHis tag was produced in *E. coli* BL21(DE3) cells. Cells were grown at 37°C in 2xYT containing antibiotics to an OD_{600} of 0.6. Protein expression was induced by 0.4 mM IPTG at 37°C for 4 h. Cells were lysed in 50 mM Tris pH 8.0 buffer containing 500 mM NaCl, 0.1%bME and 40 μl of Leupectin/Aprotin. Mcl-1 protein was purified from the soluble fraction using Ni-NTA resin (QIAGEN), following the manufacturer's instructions. The protein was further purified on a Source Q15 column (resin and column are from Amersham Biosciences) in 25 mM Tris pH 8.0 buffer, with NaCl gradient.

Fluorescence polarization-based binding assay for Bcl-2 protein

A 26-residue Bim BH3 peptide (residues 81-106: DMRPEIWIAQELRRIGDE-FNAYYARR) derived from its BH3 domain, was synthesized and labeled at the N-terminus with 6-carboxyfluorescein succinimidyl ester (FAM) as the fluorescence tag (FAM-Bim). Saturation experiments determined that FAM-Bim binds to Bcl-2 protein with a K_d value of 0.45 nM.

For competitive binding experiments, Bcl-2 protein (5 nM) and FAM-Bim peptide (1 nM) were preincubated in the assay buffer (100 mM potassium phosphate, pH 7.5; 100 μg/ml bovine gamma globulin; 0.02% sodium azide, purchased from Invitrogen, Life Technologies). 5 μl of a solution in DMSO of the tested compound was added to the Bcl-2/FAM-Bim solution in Dynex 96-well, black, round-bottom plates (Fisher Scientific) to produce a final volume of 125 μl. For each experiment, a control containing Bcl-2 and Flu-Bim peptide (equivalent to 0% inhibition), and another control containing only FAM-Bim, were included on each assay plate. After 4 hours incubation, the polarization values in milipolarization units (mP) were measured at an excitation wavelength at 485 nm and an emission wavelength at 530 nm using the Ultra plate reader (Tecan U.S. Inc., Research Triangle Park, NC). $IC_{50,}$ the inhibitor concentration at which 50% of the bound peptide is displaced, was determined from the plot using nonlinear least-squares analysis and curve fitting performed using GraphPad Prizm 4 software (GraphPad Software, San Diego, CA). The unlabeled Bid BH3 peptide is used as the positive control. The K_i value for each inhibitor was calculated using the equation developed for FP-based assays.[1] The computer program for calculating K_i values for FP-based assays is available free of charge at http://sw16.im.med.umich.edu/software/calc_ki/.

Fluorescence polarization-based binding assay for Bcl-xL protein

For this assay, we employed the 21-residue Bid BH3 peptide (residues 79-99: QEDIIRNIARHLAQVGDSMDR) labeled with 6-carboxyfluorescein succinimidyl ester

(FAM-Bid) instead of the FAM-Bim to maximize the signal. It was determined that FAM-Bid has a K_d value of 2.5 nM to Bcl-xL protein. The competitive binding assay for Bcl-xL was the same as that for Bcl-2 with the following exceptions: 30 nM of Bcl-xL protein and 2.5 nM of FAM-Bid peptide were used in the assay buffer, which consisted of 50 mM Tris-Bis, pH 7.4 and 0.01% bovine gamma globulin.

Fluorescence polarization-based binding assay for Mcl-1 protein

FAM-Bim peptide and human Mcl-1 protein were used. It was determined that FAM-Bim peptide binds to human Mcl-1 protein with a K_d value of 0.22 nM. The competitive binding assays for Mcl-1 were performed in the same manner as that for Bcl-2 with the following exceptions: 2 nM Mcl-1 and 1 nM Flu-Bim peptide were used in an assay buffer of 100 mM potassium phosphate, pH 7.5; 100 μg/ml bovine gamma globulin; 0.02% sodium azide, purchased from Invitrogen, Life Technologies.

III. Molecular modeling

Docking simulations of the designed inhibitors with the Mcl-1 and Bcl-2 proteins.

In the binding model prediction between the compounds with Bcl-2, the same protocol used in our previous study was employed.[1] The three-dimensional structure of Mcl-1 used for docking simulation was taken from the complex structure between human Mcl-1 and mNoxa (PDB entry: 2NLA).[3] Although the complex structure between human Mcl-1 and human Bim was available (PDB entry: 2NL9), one MET was replaced with MSE for crystallographic purpose and the structure of human Mcl-1 is incomplete compared with that in 2NLA. For our later stage MD refinement, we used the Mcl-1 structure from 2NLA for docking simulation and compared the binding model with the structure between human Mcl-1 and human Bim via alignment of both structures of Mcl-1.

All the docking simulations were performed using GOLD (version 2.2.)[4] The designed compounds were sketched and minimized using the Sybyl program.[5] The center of the binding site of Mcl-1 was set at Phe228 and the radius of the binding site was defined as 13 Å, large enough to cover the putative binding pocket. For each genetic algorithm (GA) run, a maximum number of 200,000 operations were performed on a population of 5 islands of 100 individuals. Operator weights for crossover, mutation and migration were set to 95, 95 and 10 respectively. The docking was terminated after 20 runs for each inhibitor. ChemScore, implemented in the Gold program, was used as the fitness function to evaluate the docked conformations. Twenty highest ranked conformations by the fitness function were saved as predicted docking modes for

analysis. The highest ranked docked conformation of the compound **4** and similar pose of compound **2** selected by the ChemScore fitness function with Bcl-2 were shown in **Figure 2** in the main body of the manuscript as the predicted binding models. The binding model with compound 4 in complex with Mcl-1 was shown as Figure 5 in the main body of the manuscript.

*Molecular dynamics simulations of the binding models between compound **4** and Bcl-2 and Mcl-1 proteins.*

The charge and force field parameters of compound **4** were obtained using the most recent Antechamber module in the Amber 9 program suite,[6] where the charge model of compound **4** was calculated via the AM1-BCC model. The predicted binding models of compound **4** with Bcl-2 and Mcl-1 were then used in the molecular dynamics simulations using the Amber program.[6] Protocols for the MD simulation are the following: The total charge of the system was neutralized by first adding counter ions. Then, the system was solvated in a 10 Å cubic box of water where the TIP3P model[7] was used. 2000 steps of minimization of the system were performed where the protein and compound **7** were constrained by a force constant of 50 kcal/mol/Å^2. After minimization, a 20 ps simulation was used to gradually raise the temperature of the system to 298 K while the whole system was constrained by a force constant of 10 kcal/mol/Å^2. Another 40 ps of equilibrium run was used where only the backbone atoms of the protein and the ligand atoms were constrained by a force constant of 2 kcal/mol/Å^2. A final production run of 1 ns was performed with no constraints on any atoms of the complex structure. When applying constraints, the initial complex structure was used as a reference

structure. All the MD simulations were at NTP. The SHAKE algorithm[8] was used to fix the bonds involving hydrogen. The PME method[9] was used and the non-bonded cutoff distance was set at 10 Å. The time step was 2 fs, and neighboring pairs list was updated in every 20 steps. Final conformations of the complexes of compound **4** in complex with Bcl-2 and Mcl-1 are shown in *Figure S1,* and *Figure 4*, respectively.

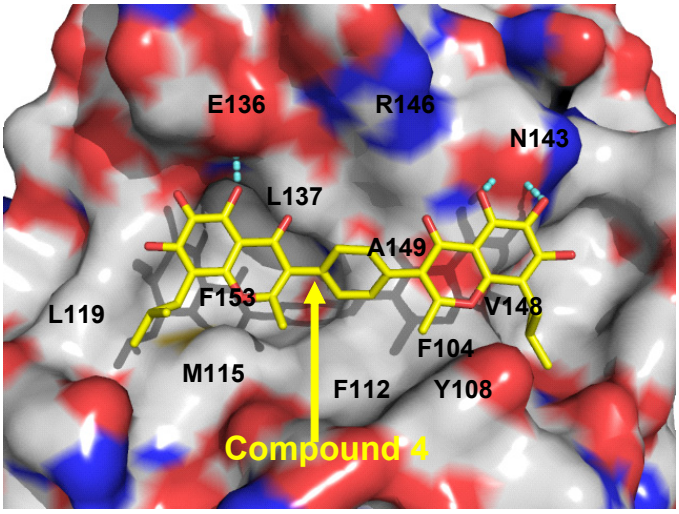

Figure S1. Predicted binding model of compound **4** with Bcl-2 obtained after a 1 ns MD simulation.

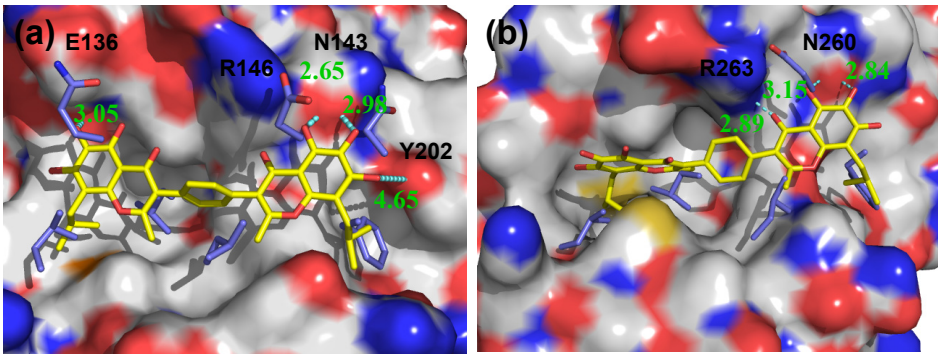

Figure S2 Predicted binding model of compound **4** with (a) Bcl-2 and (b) Mcl-1. Distances of hydrogen bonds between compound **4** and residues in Bcl-2, Mcl-1 are labled. Van der Waals contacts between residues and compound **4** (within 4 Å in distance) based on Ligplot[10] analysis for Bcl-2 are F104, R107, Y108, M115, L119, G145, A149 and F153. For Mcl-1, they include V220, H224, M231, L235, L246, V249, G262, V265, T266, F270.

V. Western blot analysis, cell growth inhibition, apoptosis and cell death induction assays

The levels of Bcl-2, Bcl-xL and Mcl-1 proteins were probed with Western blot using specific antibody against Bcl-2, Bcl-xL and Mcl-1 proteins. The protein levels of Bcl-2, Bcl-xL and Mcl-1 in the MDA-MB-231 (2LMP) human breast cancer cell line, normal prostate epithelial cells (PrEC) and normal WI-38 fibroblast cells are shown in ***Figure S3***.

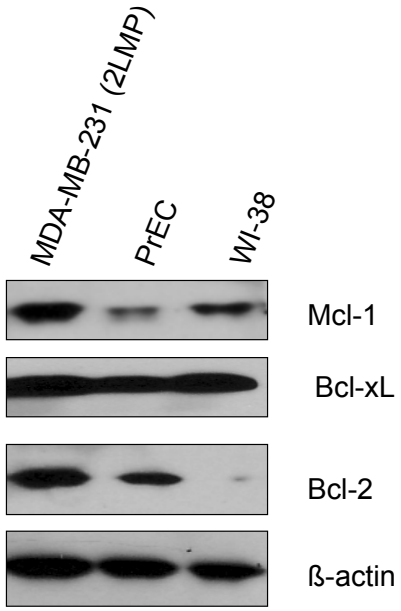

Figure S3. Western blot analysis of the basal levels of Bcl-2, Bcl-xL and Mcl-1 proteins in the MDA-MB-231 human breast cancer cell line, normal prostate epithelial cells (PrEC) and normal fibroblast WI-38 cells.

Cells were seeded in 96-well flat bottom cell culture plates at a density of $3\text{-}4\times10^3$ cells/well with compounds and incubated for 4 days. The rate of cell growth inhibition after treatment with increasing concentrations of the tested compounds was determined by WST-8 (2-(2-methoxy-4-nitrophenyl)-3-(4-nitrophenyl)-5-(2,4-disulfophenyl)-2H-

tetrazolium monosodium salt (Dojindo Molecular Technologies Inc., Gaithersburg, Maryland). WST-8 was added at a final concentration of 10% to each well, and then the plates were incubated at 37°C for 2-3 hrs. The absorbance of the samples was measured at 450 nm using a TECAN ULTRA Reader. Concentration of the compounds that inhibited cell growth by 50% (IC_{50}) was calculated by comparing absorbance in the untreated cells and the cells treated with the compounds.

For apoptosis analysis, an Annexin-V-FLUOS/Propidium iodide (PI) staining kit (Roche Applied Science) was used according to the manufacturer's instructions. Early stage apoptotic cells display translocation of phosphatidylserine from the inner to the outer surface of the plasma membrane which can be detected by annexin V fluorescein staining. Cells were treated for three days with our compounds, then harvested, washed with PBS and stained at room temperature with annexin V and PI. Cells were acquired and analyzed in a flow cytometer. Annexin V (+) /PI (-) and Annexin V (+)/PI (+) cells were scored as early and late apoptotic cells, respectively.

Trypan blue exclusion assay was used for determination of cell viability. Cells were treated with compounds **4** and **5** for 24, 48 or 96 hours. Cell viability was determined using the Trypan blue exclusion assay. Blue cells or morphologically unhealthy cells were scored as dead cells. At least 50 cells from each treatment, performed in triplicate, were counted.

References

1. Nikolovska-Coleska, Z.; Wang, R.; Fang, X.; Pan, H.; Tomita, Y.; Li, P.; Roller, P.P.; Krajewski, K.; Saito, N.G.; Stuckey, J.A.; Wang, S. Development and optimization of a binding assay for the XIAP BIR3 domain using fluorescence polarization. *Anal Biochem.* **2004**, *332*, 261-73.
2. Wang, G.; Nikolovska-Coleska, Z.; Yang, C.-Y.; Wang, R.; Tang, G.; Guo, J.; Shangary, S.; Qiu, S.; Gao, W.; Yang, D.; Meagher, J.; Stuckey, J.; Krajewski, K.; Jiang, S.; Roller, P. P.; Abaan, H. O.; Tomita, Y.; Wang, S. Structure-Based Design of Potent Small-Molecule Inhibitors of Anti-Apoptotic Bcl-2 Proteins *J. Med. Chem.*, **2006**, *49*, 6139-6142.
3. Berman, H. M.; Westbrook, J.; Feng, Z.; Gilliland, G; Bhat, T. N.; Weissig, H.; Shindyalov, I. N.; Bourne, P. E. The Protein Data Bank. *Nucleic Acids Res.* **2002,** *28*, 235-242. (www.rcsb.org/pdb/).
4. Jones, G.; Willett, P.; Glen, R. C.; Leach, A. R.; Talylor, R., Development and validation of a genetic algorithm for flexible docking. *J. Mol. Biol.* **1997**, 267, 727-748.
5. Sybyl, a molecular modeling system, is supplied by Tripos, Inc., St. Louis, MO 63144.
6. Case, D. A.; Darden, T. E.; Cheatham III, C. L.; Simmerling, J.; Wang, J.; Duke, R. E.; Luo, R.; Merz, K. M.; Pearlman, D. A.; Crowley, M.; Walker, R. C.; Zhang, W.; Wang, B.; Hayik, S.; Roitberg, A.; Seabra, G.; Wong, K. F; Paesani, F.; Wu, X.; Brozell, S.; Tsui, V.; Gohlke, H.; Yang, L.; Tan, C.; Mongan, J.; Hornak, V.;

Cui, G.; Beroza, P.; Mathews, D. H.; Schafmeister, C.; Ross, W. S.; Kollman, P. A., (2006), AMBER9, University of California, San Francisco.

7. Jorgensen, W. L.; Chandrasekhar, J.; Madura, J. D.; Impey, W. R.; Klein, M. L., Comparison of simple potential functions for simulating liquid water. *J. Chem. Phys*. **1983**, *79*, 926-935.
8. Rychaert, J. P.; Ciccotti, G.; Berendsen, H. C. J., Numerical integration of the Cartesian equations of motion of a system with constraints: Molecular dynamics of n-alkanes. *J. Comput. Phys*. **1997**, *23*, 327-341.
9. Darden, T. A.; York, D. M.; Pedersen, L., Particle mesh Ewald—an Nlog(N) method for Ewald sums in large systems. *J. Chem. Phys*. **1993**, *98*, 10089-10092.
10. Wallace, A. C.; Laskowski, R. A.; Thornton, J. M., LIGPLOT: A program to generate schematic diagrams of protein-ligand interactions. *Prot. Eng.*, **1995**, *8*, 127-134.